Evidence for loss of protons and octahedral iron from oxidized biotites and vermiculites

V. C. FARMER, J. D. RUSSELL, AND W. J. McHARDY

The Macaulay Institute for Soil Research, Craigiebuckler, Aberdeen, Scotland

A. C. D. NEWMAN

Pedology Department, Rothamsted Experimental Station, Harpenden, Herts.

J. L. AHLRICHS

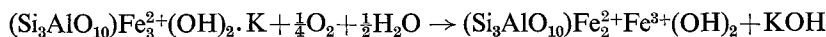Purdue University, Lafayette, Indiana, U.S.A.

J. Y. H. RIMSAITE

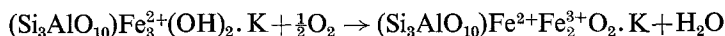Geology Survey of Canada, Ottawa, Canada

SUMMARY. Infra-red examination of a weathered biotite and of biotites that have been converted to vermiculites and subsequently oxidized, indicates that oxidation of octahedral ferrous ions to ferric ions is associated with a reversible conversion of hydroxyl ions to oxide ions. Subsequently, in high-iron biotites, there is an irreversible loss of ferric ions from the octahedral layer, resulting in an increased number of dioctahedral sites. Electron microscopy and X-ray diffraction indicate that ejected ferric ions form either amorphous interlayer oxides or, when bromine is used as an oxidant, a crystalline external phase of β-FeOOH. The high refractive index of some oxidized vermiculites is shown to be due largely to submicroscopic iron oxides.

IRON in fresh biotites is predominantly in the ferrous form, but natural weathering processes in soils or fractured rocks can largely oxidize this iron to the ferric state, with or without accompanying vermiculitization of the biotite. This change in valency must be compensated by other changes in the biotite, and three possible mechanisms have been postulated, which are formulated below for the ferrous end member (annite) of the phlogopite–biotite series:
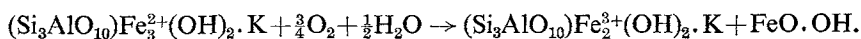
loss of interlayer cations

$$(Si_3AlO_{10})Fe_3^{2+}(OH)_2 \cdot K + \tfrac{1}{4}O_2 + \tfrac{1}{2}H_2O \rightarrow (Si_3AlO_{10})Fe_2^{2+}Fe^{3+}(OH)_2 + KOH$$

loss of hydroxyl protons

$$(Si_3AlO_{10})Fe_3^{2+}(OH)_2 \cdot K + \tfrac{1}{2}O_2 \rightarrow (Si_3AlO_{10})Fe^{2+}Fe_2^{3+}O_2 \cdot K + H_2O$$

loss of octahedral iron

$$(Si_3AlO_{10})Fe_3^{2+}(OH)_2 \cdot K + \tfrac{3}{4}O_2 + \tfrac{1}{2}H_2O \rightarrow (Si_3AlO_{10})Fe_2^{3+}(OH)_2 \cdot K + FeO \cdot OH.$$

The first of these can play at most only a minor role in high-iron biotites, as the amount of iron oxidized during vermiculitization is very much greater than the decrease in layer charge (see, for example, Newman and Brown, 1966).

The second mechanism, involving conversion of hydroxyl to oxide ions, has been well established for thermal oxidation of biotites. Indeed, in an inert atmosphere at 500–900 °C auto-oxidation occurs and hydrogen is liberated (Tsvetkov and Val'yashi-khina, 1956). It is less certain that this mechanism is implicated in oxidative weathering, as the excess water always present is difficult to distinguish from constitutional hydroxyl (Rimsaite, 1967, 1970; Newman and Brown, 1966).

The third mechanism, involving formation of iron oxides, was discounted by Wones (1963) in his hydrothermal study of interconversions between annite and oxyannite on the grounds that the oxidation–reduction process was reversible, and no discrete iron oxide phase was detectable. Separation of hematite during hydrothermal oxidation of natural biotites was, however, observed by Hellner and Euler (1957) to begin at 350 °C, without breakdown of the biotite. Loss of octahedral iron has also been postulated as occurring at ambient temperatures in soils to account for the lower iron content of weathered oxidized biotites and vermiculites compared with the fresh biotites from the parent rock (Walker, 1949; Wilson, 1970). Rimsaite (1967), however, has described biotites, high in iron, in which oxidation has occurred without significant change in the total iron content and where no separate iron oxide phase could be detected. Although calculated formulae for these oxidized biotites indicated more octahedral vacancies than in the unoxidized biotites, this was a direct result of the assumption that the total anion charge in the unit cell was unchanged. Since Fe^{2+} is oxidized to Fe^{3+}, fewer cations are required to satisfy the 44 negative charges per unit cell, and the deficit appears as vacancies in the octahedral layer. When the formulae of these oxidized biotites are recalculated on the basis of $44 + z$ anionic and cationic charges in the unit cell, where z is the charge difference between the parent and altered micas (Rimsaite, 1970), there is apparently no increase in octahedral vacancies. But these formulae will also be in error if the oxidized biotites contain a submicroscopic iron oxide phase in their interlayer spaces.

In view of the difficulties in interpreting chemical analyses, an infra-red study of biotites, oxidized naturally or in the laboratory, has been undertaken. Infra-red spectra show the vibrations of hydroxyl groups, and should permit observation of loss of hydroxyl, as in the second mechanism above, or change in the co-ordination of hydroxyl, as in the third. Some preliminary results, giving evidence for loss of octahedral iron, have been published (Farmer, Russell, Ahlrichs, and Velde, 1967). Hydroxyl absorption in thermally oxidized biotites has been studied by Vedder and Wilkins (1969).

Materials and methods

Biotites. Several biotites that have been the subject of previous studies have been used in the present work. These included a biotite crystal of which part has been weathered and oxidized, resulting in a change from dark green to gold, from the same locality as biotites 44 and 45 described by Rimsaite (1967, 1970), and also a larger

sample of a similar fresh green biotite (31A), from the same area. Professor Fripiat kindly supplied the Luindi I biotite used in the work of Fripiat, Rouxhet, and Jacobs (1965). The analysed biotites M2 to M5 and their hydrated sodium forms (AM2 to AM5), studied by Newman and Brown (1966), were also examined, together with a biotite (536) of high octahedral aluminium content (Farmer et al., 1967).

Conversion of biotites to vermiculites. Thin flakes of biotite 31A and Luindi biotite were broken down to sub-millimetre size in water suspension in a Waring Blender. Interlayer potassium ions were then replaced by hydrated barium ions by refluxing 5 g of the biotites with 1 l of 0·05 M $BaCl_2$ solution, changing the solution each day (Rausell-Colom et al., 1965). Two to three weeks' treatment was necessary to reduce the potassium content to less than 0·5 %. Refluxing the products with 1 M NaCl solution (4 treatments of 1 h with fresh solution) replaced the interlayer barium with sodium ions. These hydrated forms, giving 12·1 Å 001 spacings, are here termed vermiculites or altered biotites to distinguish them from the original biotites. Smaller amounts of other biotites were also vermiculitized by this technique.

Oxidation of vermiculites. The dark green or olive-brown vermiculites were oxidized to orange-yellow or golden forms by two techniques: heating on the water-bath for 1 h with H_2O_2, which gave a very bulky product because of exfoliation by liberated oxygen; and immersion in bromine water in a closed vessel, the water being kept saturated by diffusion of vapour from a pool of bromine in a separate beaker. Oxidation to a golden form took one to two weeks, but left the flakes compact.

The oxidized vermiculites were then refluxed with 1 M NaCl solutions to ensure that sodium occupied all exchange sites.

Reduction of oxidized vermiculites. Two techniques were used: immersion in hydrazine hydrate in a closed vessel; and repeated treatment with sodium dithionite in citrate buffered solutions, by the method of Mehra and Jackson (1960) for removing iron oxides from clays.

Chemical analysis. 10–25 mg of biotites and vermiculites were dissolved by evaporation with sulphuric and hydrofluoric acids until fuming. Sodium and potassium contents of the solutions were determined by emission flame photometry using an air:acetylene flame, and magnesium similarly, using a nitrous oxide:butane flame; total iron contents were determined colorimetrically using 1,10-phenanthroline, following Sandell (1959). Ferrous iron contents were determined on separate samples (10 mg) brought into solution with sulphuric and hydrofluoric acids, under flowing CO_2, followed by conversion of the hydrofluoric to fluoroboric acid (a micro-modification of the procedure described by Washington, 1930). Ferrous iron was determined colorimetrically following the procedure of Pollock and Miguel (1967) using 4,7-diphenyl-1,10-phenanthroline. Standard curves were prepared from ferrous ammonium sulphate solutions given the same treatment as the samples, including digestion with $HF–H_2SO_4$.

Total iron in dithionite–citrate extracts was determined by the 1,10-phenanthroline

procedure after destroying excess reagents by evaporation of aliquots to dryness with nitric acid, followed by evaporation to dryness with hydrochloric acid to destroy nitrate ion.

Instrumental procedures. Infra-red spectra were recorded on a Grubb–Parsons Spectromaster. Samples were generally dispersed in KBr discs, but films prepared from dispersions of propylammonium-saturated vermiculites were also used (Farmer, Russell, and Ahlrichs, 1968). X-ray diffraction results were obtained with a Philips diffractometer, and electron micrographs with a A.E.I. EM6 instrument.

For electron microscopy small samples of the treated biotites were subjected to 5 min mild ultrasonic treatment in water, and then centrifuged for 30 s or allowed to stand for several hours, when drops of the supernatant fluids had to be diluted to give a suitably dispersed specimen. Platinum carbon replicas of freshly cleaved flakes of the weathered biotite were prepared using a method similar to that described by Roth *et al.* (1967).

Results and interpretation

Fresh biotites

Hydroxyl groups that are co-ordinated to three octahedral cations are oriented nearly perpendicularly to the layers, and give hydroxyl absorption in the range

3640 cm^{-1} to 3705 cm^{-1}, which increases in intensity when biotite flakes are turned at an angle to the infra-red beam (see fig. 1). The vibrational frequency of these hydroxyl groups is determined by the octahedral cations to which they are co-ordinated, by the interlayer cations, and by other factors that are not fully understood (Vedder, 1964; Wilkins, 1967; Vedder and Wilkins, 1969; Farmer and Russell, 1966). The individual components of the absorption band are often unresolved, but the maximum of the composite absorption shifts to lower frequency with increasing octahedral ferrous ion content of the biotite.

Biotites commonly have vacant sites in their octahedral layer, so that some hydroxyl groups are co-ordinated to only two cations. These hydroxyl groups are oriented nearly parallel to the layers and give absorption bands in the region
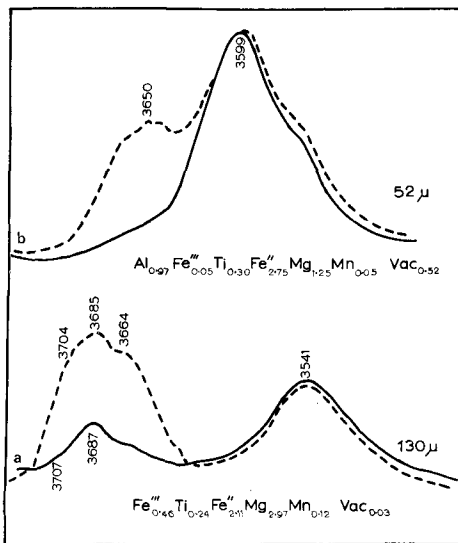
FIG. 1. Hydroxyl absorption of (*a*) biotite M4 and (*b*) biotite 536, with the flake perpendicular to the beam (full line) and at 45° to the beam (dashed line).

3620 cm^{-1} to 3540 cm^{-1} (vacancy bands), which are not affected by the orientation of the silicate sheets relative to the beam. Up to three bands may be resolved in this region, at 3620 cm^{-1}, 3600 to 3590 cm^{-1}, and 3560 to 3540 cm^{-1}. Vedder (1964) has suggested

that these bands be ascribed to hydroxyl associated with $R^{2+}R^{2+}$, $R^{2+}R^{3+}$, and $R^{3+}R^{3+}$ octahedral pairs, respectively, where R^{2+} represents Mg^{2+} or Fe^{2+}, and R^{3+} represents Al^{3+} or Fe^{3+}. Such an assignment is inconsistent with the spectrum of biotite M4 (fig. 1), in which only the lowest frequency band appears, but in which the probability of $R^{3+}R^{3+}$ pairs is very low. A more satisfactory assignment (Farmer *et al.*, 1967) arises from the observations (fig. 1) that biotite M4, for which the only vacancy hydroxyl absorption lies at 3541 cm^{-1}, contains octahedral Fe^{3+} but no octahedral Al^{3+}, whereas biotite 536 in which the band at 3599 cm^{-1} predominates, contains considerably more Al^{3+} than Fe^{3+} in its octahedral layer. Since these bands become intense only when the ferrous content is high, they are ascribed to hydroxyl associated with $Fe^{2+}Fe^{3+}$ and $Fe^{2+}Al^{3+}$ pairs, respectively. The vacancy band at 3620 cm^{-1} is never strong, and predominates only in biotites with moderate ferrous contents. As it is always associated with a band at 3590–3600 cm^{-1} it might plausibly be ascribed to hydroxyl co-ordinated to $MgAl^{3+}$. The assignments proposed above are qualitatively consistent with the spectra of fourteen analysed biotites and phlogopites that have been examined.

Oxidized biotites and vermiculites

When biotites were converted to vermiculites by refluxing successively in $BaCl_2$ and NaCl solutions, the hydroxyl absorption pattern did not change, and analyses (table I) showed little oxidation of ferrous ions. Significant oxidation by air does occur during the slower replacement of interlayer potassium by treatment at room temperature with sodium tetraphenyl boron solution (Newman and Brown, 1966) or with frequently changed sodium chloride solutions, and this oxidation affects principally the bands of hydroxyl of filled sites. More vigorous oxidation of these vermiculites with hydrogen peroxide or bromine causes a marked development of hydroxyl absorption in the region of the vacancy bands.

The implications of these changes in absorption of hydroxyl on trioctahedral and dioctahedral sites will be discussed separately.

Hydroxyl on trioctahedral sites. The shift to lower frequencies in the maximum of the trioctahedral hydroxyl absorption that occurs during preparation of the sodium-altered micas from biotites M4 and M5 (figs. 2b and 3b) can be ascribed to the partial conversion of ferrous ions to ferric ions, and a consequent change in the vibrational frequency of associated hydroxyl groups. This change is almost completely reversed (figs. 2c and 3c) when these altered micas are reduced with hydrazine, which is known to be effective in reducing octahedral ferric ions in smectites (Farmer *et al.*, 1967). When these biotites are fully oxidized with hydrogen peroxide, the changes in spectra can no longer be completely reversed by hydrazine (fig. 3d, e); hydroxyl absorption is regenerated but at a lower frequency than in the original biotite, indicating that some of the ferric ions formed in the octahedral layer can no longer be reduced.

These oxidation–reduction reactions might be expected to be associated with changes in the number of hydroxyl groups, according to the equations
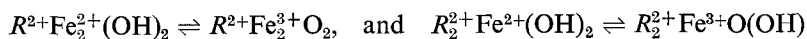
$$R^{2+}Fe_2^{2+}(OH)_2 \rightleftharpoons R^{2+}Fe_2^{3+}O_2, \quad \text{and} \quad R_2^{2+}Fe^{2+}(OH)_2 \rightleftharpoons R_2^{2+}Fe^{3+}O(OH)$$

TABLE I. *Characteristics of biotites and vermiculites; exchange capacities and element contents are based on ignited weights*

	Interlayer cations* m. eq./100 g	Fe^{2+}	$Fe^{2+}+Fe^{3+}$	Mg	Refractive index (γ)	d_{001}†	d_{060}†
Biotite 31A							
Na-form, unoxidized	222	20·0 %	23·7 %	1·65 %	1·658	10·07 Å	9·24 Å
Na-form, Br₂ oxidized	183	18·9	23·2	1·60	1·621	10·04	9·24
Na-form, Br₂ oxidized	180	<0·1	24·6	n.d.	~1·73	10·24	9·12
Na-form, Br₂ oxidized then reduced	193	3·6	22·0	1·55	1·665	10·20	9·19
Biotite, Luindi							
Na-form, unoxidized	219	16·7	21·7	5·40	1·658	10·05	9·26
Na-form, Br₂ oxidized	182	13·5	20·4	5·50	1·620	10·02	9·26
Na-form, Br₂ oxidized	181	<0·1	20·8	n.d.	~1·70	10·08	9·19
Na-form, Br₂ oxidized then reduced	198	3·0	18·5	5·40	1·657	10·08	9·20

* $Na^+ + K^+$, recalculated to correspond to K^+-saturated forms, to allow for the different contributions of Na^+ and K^+ to the formula weights.

† Vermiculites were K^+-saturated and heated to 100° before X-ray examination.

n.d. Not determined.

where R^{2+} represents Mg^{2+} or Fe^{2+}; but quantitative conclusions cannot be drawn from figs. 2 and 3, because of uncertainties about the absorptivity of the different types of hydroxyl group, and difficulties in obtaining quantitative measurements by the pressed-disc technique used. Unambiguous evidence for loss and recovery of hydroxyl was, however, obtained using a film prepared from a dispersion of the high-iron vermiculite 31A (fig. 4). Air oxidation of the suspension had led to almost total
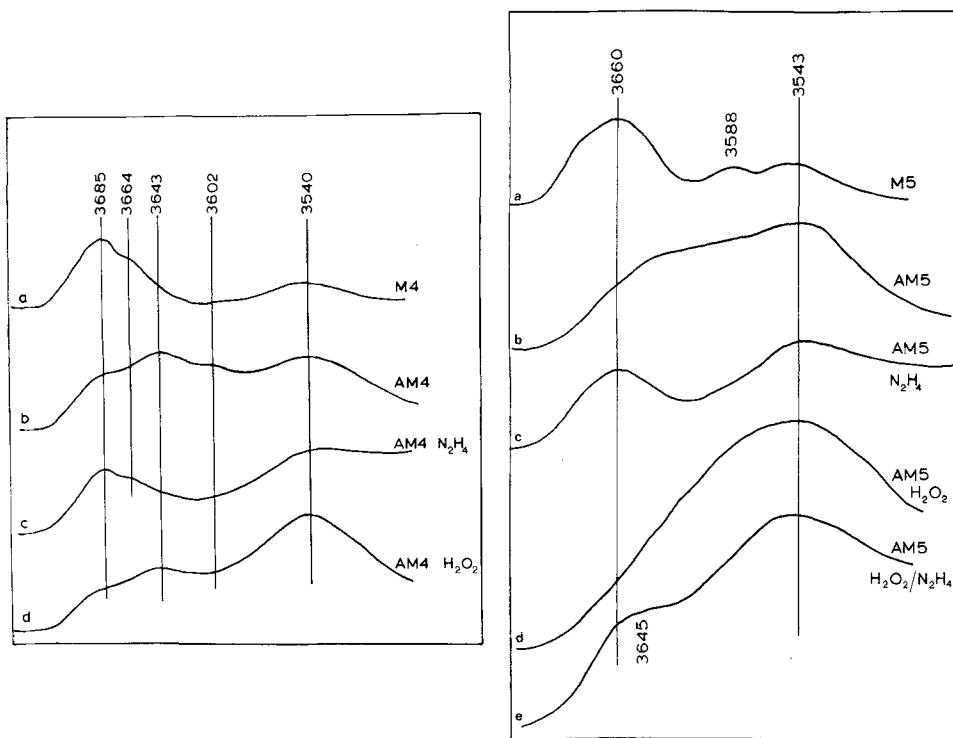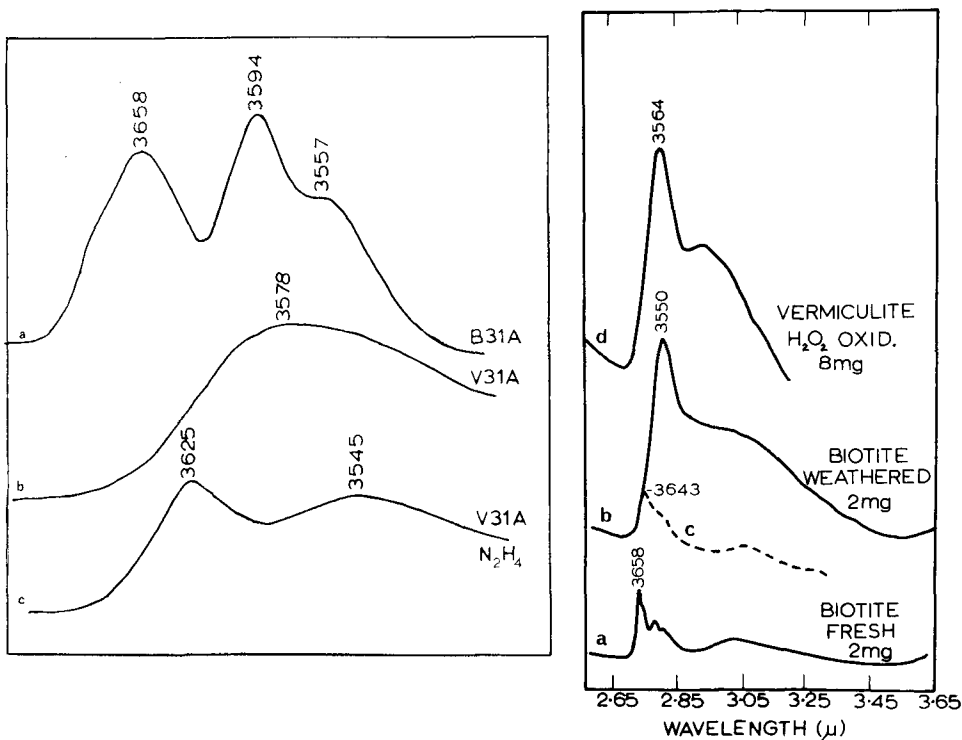

FIGS. 2 and 3: Fig. 2 (left). Hydroxyl absorption of (a) biotite M4, (b) Na-altered M4 (AM4), (c) AM4 treated with hydrazine for 7 days, and (d) AM4 oxidized with H_2O_2. 10 mg samples dispersed in KBr discs (12 mm diameter) and discs heated to 200 °C. Fig. 3 (right). Hydroxyl absorption of (a) biotite M5, (b) Na-altered M5 (AM5), (c) AM5 treated with hydrazine for 7 days, (d) AM5 oxidized with H_2O_2, and (e) AM5 oxidized then treated with hydrazine for 7 days. 10 mg samples dispersed in KBr discs (12 mm diameter), and discs heated to 200 °C.

loss of hydroxyl on trioctahedral sites, and the development of some hydroxyl associated with vacancies, so that the film, in which the vermiculite sheets are in parallel orientation, showed no increase in hydroxyl absorption when turned at 45° to the infra-red beam (fig. 4b). After treatment with hydrazine, absorption due to hydroxyl on trioctahedral sites developed (fig. 4c), which increased markedly on turning the film at 45° to the beam.

As pointed out by Vedder and Wilkins (1969), trioctahedral sites retaining hydroxyl groups in fully oxidized biotites should be principally of the type Mg_3, Mg_2Al, or

Mg_2Fe^{3+}. The first two are known to absorb near 3700 cm^{-1} and 3660 cm^{-1} respectively (Vedder, 1964) but the third has not yet been positively identified. It should be the only type of hydroxyl to survive on trioctahedral sites in fully oxidized high-iron vermiculites and biotites, but its absorption is obscured by the strong vacancy bands that develop (e.g. fig. 3*d*).

FIGS. 4 and 5: Fig. 4 (left). Hydroxyl absorption of (*a*) flake of biotite 31A, (*b*) Na-saturated film of vermiculite 31A, and (*c*) same film after treatment with hydrazine vapour for 24 hours; all at 45° to beam. Fig. 5 (right). Hydroxyl absorption of (*a*) fresh biotite 44/45F, (*b*) naturally weathered biotite 44/45W, (*c*) weathered biotite, partially dehydroxylated at 400 °C and (*d*) vermiculite 31A oxidized with H_2O_2. Samples in KBr discs heated to 200 °C for *a*, *b*, and *d*, and to 400 °C for spectrum *c*.

Hydroxyls associated with these vacancies were found to begin to dehydroxylate at 300 °C and were generally lost by 400 °C when the samples were heated in pressed KBr discs, i.e. at temperatures considerably lower than those Vedder and Wilkins (1969) found necessary for dehydroxylation in large biotite flakes. The residual band, due to $Mg_2Fe^{3+}OH$, was found at 3640–5 cm^{-1} in all samples studied, including the naturally weathered biotite (fig. 5*c*). In oxidized vermiculites of lower iron content, such as AM2 and AM3, the 3645 cm^{-1} band could be seen superimposed on the absorption of $MgAl^{3+}OH$ at 3660 cm^{-1}, which was present in the fresh biotite, while Mg_3OH was resolved at 3703 cm^{-1}. In oxidized AM4 (fig. 2*d*), Mg_3OH absorption

appears as a weak shoulder at 3680 cm^{-1} on the side of the predominant 3645 cm^{-1} band, confirming the observation of Vedder and Wilkins (1969) that Mg_3OH groups in oxidized biotites absorb at frequencies considerably lower than those given by some phlogopites (3718 cm^{-1}).

The origin of the 3602 cm^{-1} band in vermiculite AM4 (fig. 2b) is less certain. This band is also a persistent feature of partially oxidized vermiculite 31A, before it falls to a low level at the stage of oxidation indicated in fig. 4b. Possibly it can be ascribed to $MgFe_2^{3+}OH$ groupings, which Vedder and Wilkins (1969) have suggested may persist in oxidized biotites. Certainly, a frequency near 3600 cm^{-1} seems too low to be assigned to, say, an $MgFe^{2+}Fe^{3+}OH$ grouping (Wilkins, 1967).

It should be noted that the frequencies observed for hydroxyl absorption of Na-vermiculites in KBr pressed discs (figs. 2 and 3) are directly comparable with those given by the original biotites, as interlayer Na^+ has an effect on hydroxyl frequencies similar to that of interlayer K^+, and, in any case, much of the interlayer Na^+ is replaced by K^+, by exchange with the KBr.

Hydroxyl on dioctahedral sites. The intensity of the vacancy band near 3560 cm^{-1} that develops in oxidized biotites and vermiculites is a function of the octahedral iron content of the biotites: it was too weak to be detected in the oxidized vermiculite AM3 of Newman and Brown (1966) containing 1·2 iron ions per unit cell of six octahedral sites, but was a pronounced band in oxidized AM4, containing 2·5 iron ions per unit cell (fig. 2d). The most intense vacancy bands were given by the naturally weathered biotite (fig. 5b) derived from a fresh biotite containing about 4 iron ions per unit cell, and by the laboratory-oxidized vermiculite 31A (fig. 5d) of similar iron content.

In these oxidized vermiculites, oxidation of ferrous ions is complete (table I), and the enhancement of the vacancy bands is strong evidence for ejection of octahedral iron to compensate for the change in layer charge. The strong broad vacancy band is similar to, but less intense than that of nontronite, in which $Fe_2^{3+}OH$ groupings absorb at 3564 cm^{-1} (Farmer and Russell, 1964). Some influence of octahedral Al^{3+} can be seen on the frequency of the vacancy band in oxidized vermiculites, which ranges from 3540 cm^{-1} in oxidized AM4, containing no octahedral Al^{3+}, to 3581 cm^{-1} in oxidized vermiculite 536, containing one Al^{3+} per unit cell, which would have hydroxyl groups associated with both Fe_2^{3+} sites and $AlFe^{3+}$ sites.

An estimate of the concentration of dioctahedral sites was made on the assumption that the molar absorptivity of OH on these sites was the same as that in nontronite, using pressed KBr discs of the samples, which were carefully matched to give equal intensity of Si–O absorption near 10 μm. This indicated 1·1 vacancies per six octahedral sites in the naturally weathered biotite, i.e. that over 50 % of the mica was now dioctahedral. Similar estimates for laboratory-oxidized vermiculite 31A indicated 0·95 vacancies for Br_2-oxidized material, and 0·60 vacancies for H_2O_2-oxidized material.

Iron hydroxides, formed by ferric ions ejected from the octahedral layers, are unlikely to contribute to the 3540–80 cm^{-1} vacancy band in oxidized vermiculites

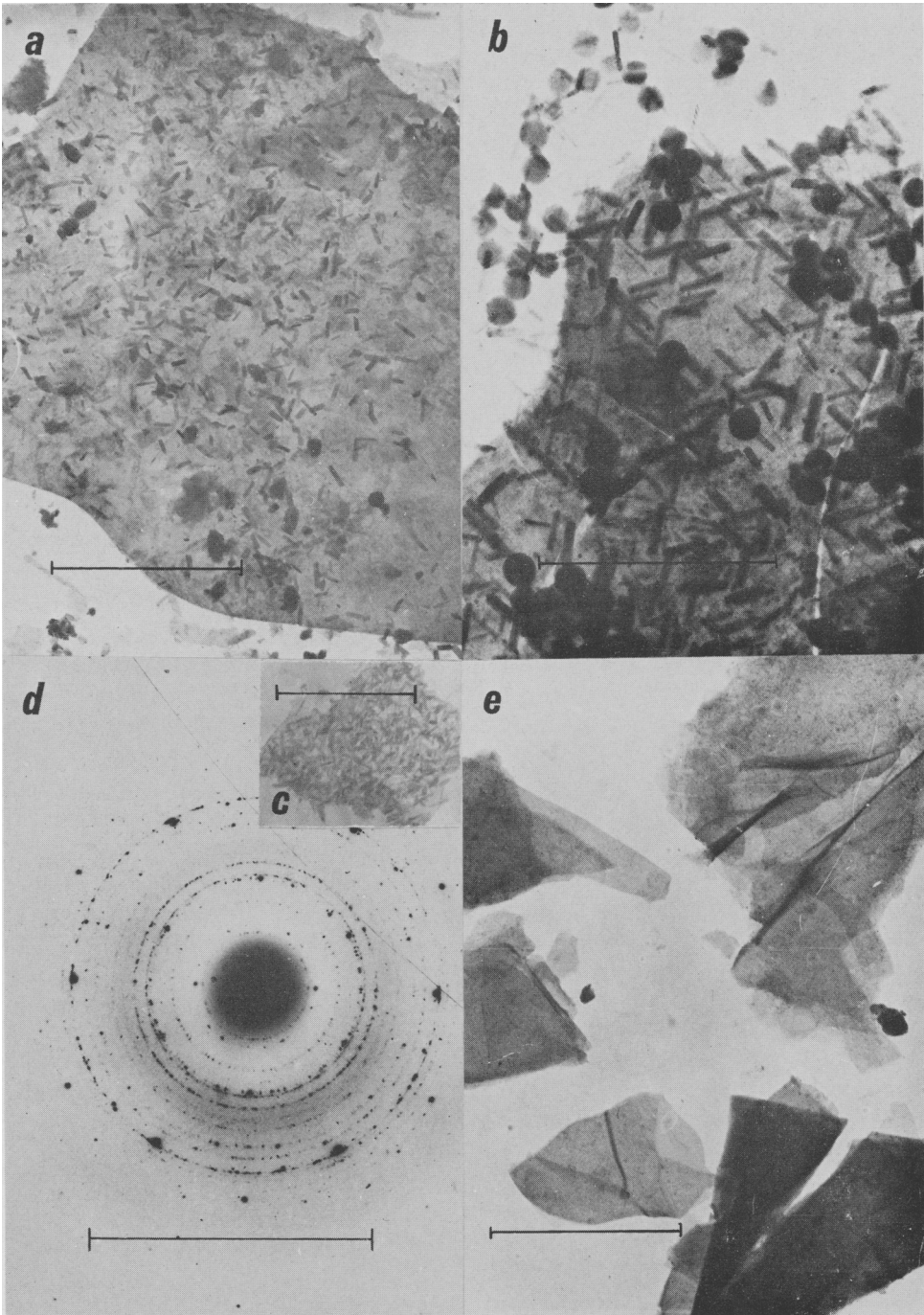FIG. 6

and biotites. A range of crystalline and amorphous iron hydroxides have been examined, and all have been found to absorb below 3370 cm^{-1}. Thus any iron hydroxides formed in the oxidized micas will probably contribute, together with adsorbed water, to the diffuse absorption on the low frequency side of the 3540 cm^{-1} band in curves b and d of fig. 5.

Electron microscopy and X-ray examination. To seek confirmation for the loss of octahedral iron, the weathered biotite and the oxidized vermiculites were examined by electron microscopy and by X-ray diffractometry. Under the electron microscope flakes of the vermiculites from biotite 31A and Luindi biotite that had been oxidized by bromine were seen to be covered with fine lath-shaped crystals (fig. 6*a*); on some flakes the crystals show preferred orientation in three directions at 120° to each other, indicating expitaxial growth on the vermiculite surface (fig. 6*b*). Where a large number of these crystals were concentrated within a small flake area as in fig. 6*c* a good polycrystalline electron diffraction pattern was obtained. Measurement of d-spacings using the underlying vermiculite pattern as a calibration proved that the laths were crystals of β–FeOOH (akaganéite). This hydroxide is known to crystallize during hydrolysis of ferric chloride solutions, and its appearance here can be ascribed to the hydrolysis of ferric bromide. The bromide ion formed within the interlayers by the reduction of bromine gives the ferric ions that have been ejected from the octahedral layer sufficient mobility to migrate out of the interlayer space, and crystallize as β–FeOOH on the surface of the crystals. Only traces of iron remained in solution following bromine oxidation, and the pH fell only to four.

No β–FeOOH was detected on vermiculites oxidized with H_2O_2; however, the vermiculite flakes had a distinctly mottled aspect indicative of the existence of very finely divided amorphous iron oxide as a separate phase within the vermiculite flake (fig. 6*e*). X-ray diffraction also indicated that the ejected ferric ions formed hydroxides within the interlayer space, increasing the 001 spacing of specimens that had been potassium-saturated and dried at 100 °C from 10 Å for unoxidized vermiculites to 11·13 Å (vermiculite 31A) and 11·42 (Luindi vermiculite) for H_2O_2-oxidized vermiculites. The basal reflections from the K-saturated unoxidized vermiculites were sharp and rational whereas those from H_2O_2-oxidized vermiculites were broad and irrational, indicative of variable interlayer spacing. The vermiculites that had been oxidized with bromine gave lower spacings (table I) than H_2O_2-oxidized material indicating that much but not all of the ejected ferric ions had migrated out of the interlayer space.

FIG. 6. (*a*) Na vermiculite from biotite 31A after bromine oxidation; ultrasonically dispersed. The marker represents 1 μm. (*b*) Na vermiculite from biotite 31A after bromine oxidation; ultrasonically dispersed. Note orientation of laths on the vermiculite flake. The spheres are 880 Å polystyrene latex particles included as magnification check. Marker represents 0·5 μm. (*c*) Mass of lath crystals from bromine-oxidized Na-vermiculite from biotite 31A giving rise to polycrystalline electron diffraction pattern in (*d*). The marker represents 1 μm. (*d*) Selected-area electron-diffraction pattern from the mass of laths in 3*c*. Apart from the 020, 040, and 060 spotty reflections from underlying vermiculite flakes, the *d* spacings agree with published X-ray data for β-FeOOH. The marker represents 1 Å^{-1}. (*e*) Na-vermiculite from biotite 31A after H_2O_2 oxidation; ultrasonically dispersed. The marker represents 1 μm.

Rimsaite (1967) reported that the naturally weathered biotite gave spacings nearly identical to those of the unweathered biotite, but that the weathered specimen gave rather diffuse reflections, which suggests the presence of interlayer deposits. Electron micrographs of surface replicas of freshly cleaved faces of weathered mica show that a large proportion of the surface is covered with fine-grained particles (fig. 7*a*). This contrasts strongly with fresh mica, which is typified by a completely smooth surface morphology with occasional sharply defined cleavage steps. At higher magnification two types of deposit can be distinguished. There are clusters of laths or tubes (fig. 7*b*) 0·2–0·4 μm long and 0·02–0·03 μm wide, and clumps of very fine-grained material (fig. 7*c*). Even relatively smooth areas of flake are peppered with fine grains. Some of the weathered mica was crushed lightly and subjected to ultrasonic dispersion so that the laths and the fine-grained material could be examined directly in the electron microscope. Fig. 7*d* shows that the particles in fig. 7*b* are extremely fragile tubes; these gave very weak electron-diffraction patterns, the strongest reflections lying along the axis of the tubes, and corresponding to the 020 and 060 planes of a dioctahedral clay mineral (d_{010} 8·95). The morphology and diffraction pattern of these tubes suggest that they are poorly crystallized halloysite. The grainy electron-dense material in fig. 7*d* corresponds to the material featured in the replica fig. 7*c*. This gave no electron diffraction and is probably amorphous iron oxide.

Selective extraction of iron. In an attempt to measure quantitatively the amount of iron liberated from the octahedral layer, oxidized vermiculites from biotite 31A and Luindi biotite were repeatedly extracted with dithionite–citrate solutions. The amounts of iron extracted from biotite 31A are shown in fig. 8. For bromine-oxidized samples there was an initial rapid solution of iron, which probably corresponds to dissolution of β–FeOOH on the surface of the crystals, followed by a continuous liberation of iron from the mica on successive extractions. Little or no surface hydroxide phase is present on H_2O_2-oxidized specimens; dissolution of iron was slower, and there was no clear break to indicate when interlayer iron hydroxides had been dissolved; nevertheless, a decrease in 001 spacings from over 11 Å to 10·2 Å (K-saturated and dried at 100 °C) does indicate that interlayer hydroxides have been at least partially extracted from H_2O_2-oxidized vermiculites. An estimate of the amount of iron liberated from octahedral sites based on the amount that is rapidly dissolved from the Br_2-oxidized samples indicates 1·8 % Fe from vermiculite 31 A and 1·0 % from Luindi vermiculite. Analysis of the residual material after eight successive extractions with dithionite–citrate (a separate experiment) indicated a loss of about 1·5–2·0 % Fe from both vermiculites (table I). A 2 % loss of iron corresponds to the development of about 0·35 vacancies per six octahedral sites, assuming no other cations are lost. Magnesium analyses indicate little loss of this ion (table I).

Some other features of the oxidized vermiculites are recorded in table I. There is some loss of layer charge during extraction of potassium, but no further change in layer charge occurs on oxidation, although the small increase following subsequent reduction with dithionite solutions is probably significant. There is a considerable increase in refractive index on oxidation of high-iron vermiculites associated with an
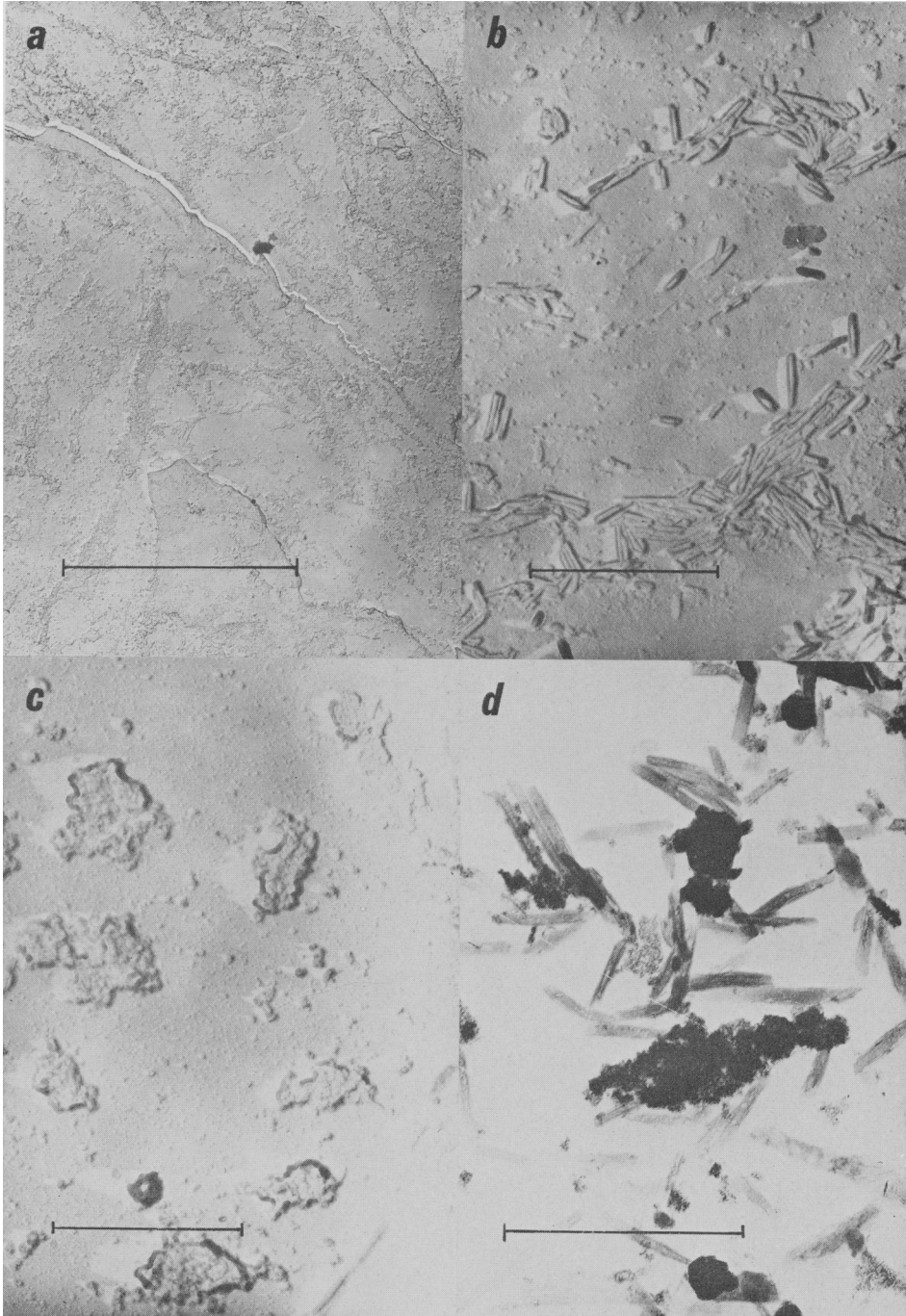
FIG. 7. (a) Naturally weathered biotite: carbon replica of freshly cleaved surface, preshadowed with Pt/C at tan⁻¹ ⅓. The marker represents 10 μm. (b) as (a). The marker represents 1 μm. (c) as (a). The marker represents 1 μm. (d) Naturally weathered biotite after light grinding and ultrasonic dispersion. The marker represents 1 μm.

increase in 2V from about 8° to 25°, similar to that observed for naturally weathered biotites (Rimsaite, 1967). For biotites of moderate iron content, there is no significant
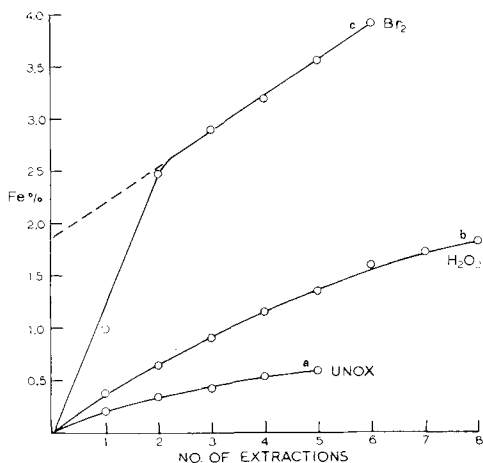

FIG. 8. Accumulated loss of Fe, on successive dithionite–citrate extractions, from vermiculite 31A: (*a*) unoxidized, (*b*) H_2O_2 oxidized, and (*c*) Br_2 oxidized.

increase of refractive index on oxidation; thus for mica M2 the γ-index of the original mica, its Na-altered form, and the H_2O_2-oxidized Na-altered form are 1·593, 1·584, and 1·582 respectively, and for mica M4 they are 1·617, 1·617, and 1·620, in contrast to M5, for which they are 1·647, 1·646, and 1·685 respectively.

It seems likely that the very high refractive indices of the oxidized vermiculites from 31A and Luindi biotites are due largely to the submicroscopic iron oxides present, as the refractive index falls substantially after dithionite extraction (table I), although 2V increases to 35–40°. Re-oxidation of the dithionite-treated vermiculites with bromine did not increase their refractive indices; this is consistent with the expectation that no further separation of iron oxides would occur.

Ignition in air at 650 °C for 20 h increased the refractive index of unoxidized vermiculite 31A to over 1·79, whereas the oxidized vermiculite that had been extracted with dithionite increased only to about 1·76 on ignition.

Oxidation also causes a decrease in the *b* dimension of the vermiculites (table I), as noted by Wones (1963) for synthetic oxybiotites, and also by Rimsaite (1967) for weathered biotites.

Discussion

The present investigation indicates that oxidation of ferrous ions in vermiculitized biotites is compensated first by a reversible loss of protons, and subsequently by an irreversible loss of octahedral iron. Loss of interlayer cations appears to play little part in the compensatory mechanism, as the decrease in layer charge on vermiculitizing the biotites is not much greater than that found by Newman (1967) for his phlogopite P3, and no further change occurs on subsequent oxidation.

In the vermiculitized biotites, the oxidizing agents (bromine, oxygen, or hydrogen peroxide) can enter the interlayer space, where electron transfer from an octahedral ferrous ion to the electron acceptor is probably mediated through a hydroxyl or oxide ion. The initial step probably involves transfer of a hydrogen atom from a hydroxyl group to the oxidant. This type of atom transfer reaction is commonly postulated for oxidation–reduction reactions in aqueous solutions (Basolo and Pearson, 1967).

At a later stage, when the remaining ferrous ions are co-ordinated only to oxide or fluoride ions, electrons may either transfer directly from oxide ions to the oxidant, or indirectly through bridging water molecules, e.g.:

$$Fe^{2+}O^{2-}\text{---}HOH\text{---}Br_2 \rightarrow Fe^{3+}O^{2-} + OH^- + HBr + Br.$$

By these mechanisms, the grouping $[Fe^{2+}Fe_2^{3+}O_2^{2-}]^{4+}$ is converted to $[Fe_3^{3+}O_2^{2-}]^{5+}$: it is suggested that the resultant local concentration of positive charge is unstable, and that a $[Fe^{3+}O^{2-}]^+$ grouping is ejected through the hexagonal holes in the silicate sheet into the interlayer space. The residual $[Fe_2^{3+}O^{2-}]^{4+}$ grouping could then rehydrate to give $[Fe_2^{3+}(OH)_2^-]^{4+}$. Although ejection of ferric ions appears to proceed more slowly than loss of protons, there is clearly no great energy barrier to this process. The marked optical anisotropy in the (001) plane of oxidized vermiculites indicates that these ions are preferentially ejected from a specific site, probably the unique site that is vacant in dioctahedral micas.

The properties of the naturally weathered biotite examined here closely match those of the laboratory-oxidized vermiculite 31A. Differences in refractive index, 2V, and hydroxyl absorption between the fresh and oxidized forms all agree. Further, changes in infra-red absorption pattern in the 10–15 μm region on weathering, not illustrated here, are closely matched by bromine oxidation of vermiculite 31A, less closely for H_2O_2-oxidized material. There can be no doubt that oxidation in nature and in the laboratory yield very similar products, although there is evidence of a further weathering process yielding small amounts of halloysite-like material in the naturally oxidized biotite. The mechanism of oxidation for the naturally weathered biotite is less obvious, as it retains a 10 Å spacing, suggesting that oxidation has proceeded without expansion of the biotite. It may be, however, that oxidation was a two-stage process, involving initial vermiculitization, followed by readsorption of potassium and collapse to 10 Å. Such a mechanism can be justified by the observation of Barshad and Kishk (1968) that oxidized vermiculites have an increased affinity for potassium. The conversion of hydroxyl to oxide ions, and the development of dioctahedral sites in which the hydroxyl groups are directed away from the interlayer cations, would both tend to increase the strength of binding of K^+ in the interlayer space. If such a process does occur readsorption of K^+ must be highly efficient, as there is little evidence for residual vermiculite layers in the weathered biotite 44W described by Rimsaite (1970). Chloritic material associated with the weathered biotite appears to be a secondary alteration product.

Wilson (1970) has presented infra-red evidence for an increase in octahedral vacancies during oxidative weathering of a biotite to hydrobiotite in soil, associated with a decrease in refractive index, and a considerable loss of iron (from 15·5 % in the fresh mica to about 10·5 % in the weathered mica). Apparently, the complexing and reducing agents present in soils can extract ejected ferric ions from the weathered mica. Walker (1949) also postulated loss of iron during weathering of a biotite in soil to an oxidized 10 Å form, and subsequently to vermiculite. His analyses show, in addition to a loss of 2 % Fe, a substantial loss of MgO (from 9·2 to 5·4 %) in the first weathering product, for which there is no analogy in the present work.

Since ejection of ferric ions from the lattice occurs so readily during oxidation at room temperature it seems highly probable that this will occur also during thermal oxidation of biotites, where blistering and delamination allow access of oxygen. The vacancies that would develop cannot be detected by infra-red spectroscopy, as the dioctahedral sites are dehydroxylated by condensation, forming water (Vedder and Wilkins, 1969). But the high refractive index of thermally oxidized biotites (Rimsaite, 1967) is evidence for interlayer submicroscopic iron oxides, in view of the finding, presented here, that oxidized vermiculites from which the liberated iron oxides have been extracted do not give such high refractive indices on heating. Similarly, it is plausible to suggest that ejection of iron from the octahedral layers occurs also for thermally oxidized amosite, where ferrous ions are oxidized in excess of the hydroxyl content and excess oxygen is taken up (Hodgson, Freeman, and Taylor, 1965*a*). Iron oxides could form in the channel containing the *A* site of amphiboles, and this migration of ferric ions might account for changes in the relative intensity of X-ray diffraction maxima during conversion of amosite to oxyamosite. In thermally oxidized crocidolite, however, there is evidence that the amount of ferrous ion that can be oxidized without breakdown of the amphibole structure is limited to one ferrous ion for each hydroxyl group (Hodgson, Freeman, and Taylor, 1965*b*; Addison, Addison, Neal, and Sharp, 1962).

One unsatisfactory feature of the present investigation is the failure to obtain a consistent estimate for the number of vacant sites that develop in oxidized vermiculites. An estimate based on the intensity of infra-red absorption by hydroxyl on dioctahedral sites indicates nearly one vacancy per six octahedral sites in oxidized vermiculite 31A, whereas the amount of iron that can be extracted by dithionite treatment indicates an increase of at most 0·3 vacancies over the unoxidized material. The number of vacancies originally present in the fresh biotite is uncertain, but appears comparable, from infra-red evidence, with the number in biotite 44F, for which Rimsaite (1970) calculates 0·3 vacancies. Obviously, some aluminium, titanium, and magnesium ions might also be ejected from the octahedral layer, although these are minor components relative to ferrous and ferric ions, and it seems likely that not all the ejected ferric ions were extracted by dithionite treatment. Even allowing for these sources of error, the discrepancy seems significant. The assumptions on which the infra-red estimate is based could well be in error; nevertheless, the higher figures given by this technique agree reasonably with the hypothesis that all $[R_3^{3+}O_2^{2-}]^{5+}$ sites are unstable, and decompose to dioctahedral sites in the oxidized micas. On this basis, and the assumption that the distribution of ions in trioctahedral sites is random, calculation indicates that the number of vacancies that would develop on oxidation of biotites 44F and 45F are 1·3 and 1·0 respectively per six octahedral sites. The infra-red estimate obtained for a weathered biotite from this locality is 1·1 vacancies. Similar calculations indicate the development of only 0·07 vacancies for oxidized AM3 (where no dioctahedral sites could be detected) and 0·25 vacancies for oxidized AM4, which showed a significant vacancy band.

REFERENCES

ADDISON (C. C.), ADDISON (W. E.), NEAL (G. H.), and SHARP (J. H.), 1962. *Journ. Chem. Soc.* 1468.

BARSHAD (I.) and KISHK (J. M.), 1968. *Science*, **162**, 1401.

BASOLO (F.) and PEARSON (R. G.), 1967. *Mechanisms of Inorganic Reactions*, 2nd edn. New York (Wiley).

FARMER (V. C.) and RUSSELL (J. D.), 1964. *Spectrochim. Acta*, **20**, 1149.

—— —— 1966. Ibid. **22**, 389.

—— —— and AHLRICHS (J. L.), 1968. *9th Int. Congr. Soil Sci., Adelaide, Australia*, **3**, 101.

—— —— —— and VELDE (B.), 1967. *Bull. Groupe franç. Argiles*, **19** (2), 5.

FRIPIAT (J. J.), ROUXHET (P.), and JACOBS (H.), 1965. *Amer. Min.* **50**, 1937.

HELLNER (E.) and EULER (R.), 1957. *Geochim. Acta.* **12**, 47.

HODGSON (A. A.), FREEMAN (A. G.), and TAYLOR (H. F. W.), 1965a. *Min. Mag.* **35**, 445.

—— —— —— 1965b. Ibid. **35**, 5.

MEHRA (O. P.) and JACKSON (M. L.), 1960. *Clays Clay Min.* **7**, 317.

NEWMAN (A. C. D.), 1967. *Clay Min.* **7**, 215.

—— and BROWN (G.), 1966. Ibid. **6**, 297.

POLLOCK (E. N.) and MIGUEL (A. H.), 1967. *Anal. Chem.* **39**, 272.

RAUSELL-COLOM (J. A.), SWEATMAN (T. R.), WELLS (C. B.), and NORRISH (K.), 1965. In *Experimental Pedology*, eds. E. G. HALLSWORTH and D. V. CRAWFORD, 40. London (Butterworth).

RIMSAITE (J.), 1967. *Clays Clay Min.* **15**, 375.

—— 1970. *Contr. Min. Petr.* **25**, 225.

ROTH (C. B.), JACKSON (M. L.), DE VILLIERS (J. M.), and VOLK (V. V.), 1967. In *Soil Chemistry and Soil Fertility*, ed. G. V. JACKS, p. 217. Trans. Meet. Comm. II & IV, int. Soc. Soil Sci., Aberdeen, 1966.

SANDELL (E. B.), 1959. *Colorimetric Determination of Traces of Metals*, 3rd edn. New York (Interscience).

[TSVETKOV (A. I.) and VAL'YASHIKHINA (E. P.)] Цветков (А. И.) и Вапьяшихина (Е. П.), 1956. Изв. Акад. наук СССР, сер. геол. (*Bull. Acad. Sci. URSS, sér. géol.*), **5**, 74.

VEDDER (W.), 1964. *Amer. Min.* **49**, 736.

—— and WILKINS (R. W. T.), 1969. Ibid. **54**, 482.

WALKER (G. F.), 1949. *Min. Mag.* **28**, 693.

WASHINGTON (H. S.), 1930. *The Chemical Analysis of Rocks*, 4th edn. New York (Wiley).

WILKINS (R. W. T.), 1967. *Min. Mag.* **36**, 325.

WILSON (M. J.), 1970. *Clay Min.* **8**, 291.

WONES (D. R.), 1963. *Amer. Min.* **48**, 1300.